

Electronic Supplementary Information

Microwave assisted *N*-alkylation of amine functionalized crystal-like mesoporous phenylene-silica

Mirtha A. O. Lourenço,^a Renée Siegel,^b Luís Mafra^b and Paula Ferreira ^{*a}

^aDepartment of Materials & Ceramics Engineering, CICECO, University of Aveiro, 3810-193 Aveiro, Portugal

^bDepartment of Chemistry, CICECO, University of Aveiro, 3810-193 Aveiro, Portugal

*Corresponding authors: pcferreira@ua.pt, +351 234401419, Fax: +351 234401470

Table of Contents

1. Experimental - characterization procedure

2. Characterization of PMO materials

Figure S1. X-ray diffraction patterns of PMO, NH₂-PMO, Alk-NH-PMO1 and Alk-NH-PMO2.

Table S1. Texture parameters of PMO, NH₂-PMO, Alk-NH-PMO1 and Alk-NH-PMO2.

Figure S2. TEM images of PMO, NH₂-PMO, Alk-NH-PMO1 and Alk-NH-PMO2.

Figure S3. -196 °C nitrogen adsorption-desorption isotherms of PMO, NH₂-PMO, Alk-NH-PMO1 and Alk-NH-PMO2.

Figure S4. ²⁹Si MAS (left) and CP-MAS (right) NMR spectra of PMO, NH₂-PMO, Alk-NH-PMO1 and Alk-NH-PMO2.

Figure S5. FTIR (ATR) spectra of PMO, NH₂-PMO, Alk-NH-PMO1 and Alk-NH-PMO2.

Table S2. Elemental analyses of PMO, NH₂-PMO, Alk-NH-PMO1 and Alk-NH-PMO2.

Figure S6. TGA of PMO, NH₂-PMO, Alk-NH-PMO1 and Alk-NH-PMO2.

1. Experimental - characterization

Transmission electron microscopy (TEM) images were recorded by a 200 kV Hitachi H8100 Instrument and by a 200 kV High Resolution (HR) and energy-filtered (EF) TEM JEOL 2200FS Instrument.

Powder X-ray diffraction (PXRD) data were collected with a Phillips X’Pert MPD diffractometer using Cu-K α radiation.

Nitrogen adsorption-desorption isotherms were recorded at -196 °C using a Gemini V 2.00 instrument model 2380. Functionalized PMO materials were dehydrated overnight at 150 °C to an ultimate pressure of 1024 mbar and then cooled to room temperature prior to adsorption.

^{13}C , ^{29}Si and ^{15}N NMR spectra were recorded using a double resonance MAS probe on a Bruker Avance III 400 spectrometer operating at 9.4 T. ^{13}C cross-polarization magic-angle spinning (CP MAS) NMR spectra were collected using the following parameters: 4 μs ^1H 90° pulse; contact time (CT): 1 ms; v_1^{H} : 70 kHz and v_1^{C} : 78 kHz for CT pulses; MAS rate (v_R): 8 kHz and recycle delay (RD): 4 s. TPPM decoupling during the acquisition of the ^{13}C signal was employed using a pulse length of 4.5 μs (ca. 165° pulses) for the basic unit block. ^{29}Si MAS NMR spectra were collected employing a 40° flip angle pulse; v_R : 5 kHz; RD: 60 s. ^{29}Si CP MAS NMR spectra were acquired with a 4 μs ^1H 90° pulse; CT: 8 ms, v_R : 5 kHz; RD: 5 s. ^{15}N CP MAS NMR spectra were recorded using a 4 μs ^1H 90° flip angle pulse; v_1^{H} : 57.7 kHz and v_1^{N} : 62.5 kHz for CT pulses; CT: 8 ms; v_R : 5 kHz and RD: 5 s. In both ^{29}Si and ^{15}N NMR experiments a CW decoupling rf field strength of 53 kHz was applied during the acquisition time. In all the CPMAS experiments, the ^1H rf field strengths used during the CT pulse were ramped from 50% to 100% to improve CP stability.

The ^{13}C and ^{29}Si NMR spectra were quoted in ppm from trimethylsilane, while ^{15}N NMR spectra were referenced against a solid sample of natural abundance L-glycine, a secondary reference standard with respect to nitromethane.

Thermogravimetric analysis (TGA) was carried out on a Shimadzu TGA-50 instrument with a program rate of 5 °C min $^{-1}$ in air.

Fourier transform infrared (FTIR) was done in a FTIR Bruker Tensor 27 instrument with a Golden Gate ATR (Attenuated Total Reflectance). Mesoporous powders were dehydrated at 100 °C for 24 h before FTIR analysis. The FTIR spectra were recorded in transmittance mode.

Elemental analysis was carried out in C.A.C.T.I. in the Vigo University.

2. Characterization PMO materials

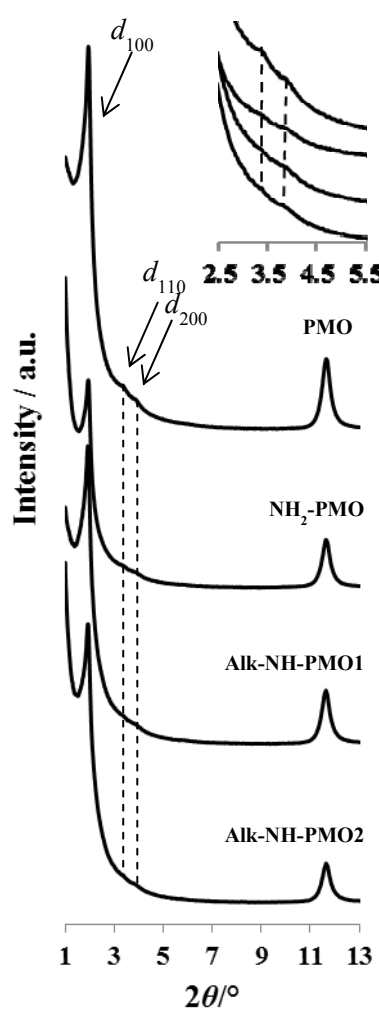


Figure S1. X-ray diffraction patterns of PMO, NH₂-PMO, Alk-NH-PMO1 and Alk-NH-PMO2. The inset displays the magnified patterns in the 2θ region from 2.5 to 5.5°.

Table S1. Physical properties of PMO, NH₂-PMO, Alk-NH-PMO1 and Alk-NH-PMO2.

Sample	d_{100} / nm	S_{BET} / m ² g ⁻¹	V_p / cm ³ g ⁻¹	d_p / nm ^a	b / nm ^b
PMO	4.48	782	0.63	3.55	1.62
NH ₂ -PMO	4.53	719	0.51	3.55	1.68
Alk-NH-PMO1	4.53	693	0.50	3.41	1.82
Alk-NH-PMO2	4.53	698	0.53	3.41	1.82

^aPore width obtained from the maximum on the BJH pore size distribution calculated on the basis of adsorption data. ^bPore wall thickness calculated as $(2d_{100}/\sqrt{3} - d_p)$, where the first term is the unit cell parameter.

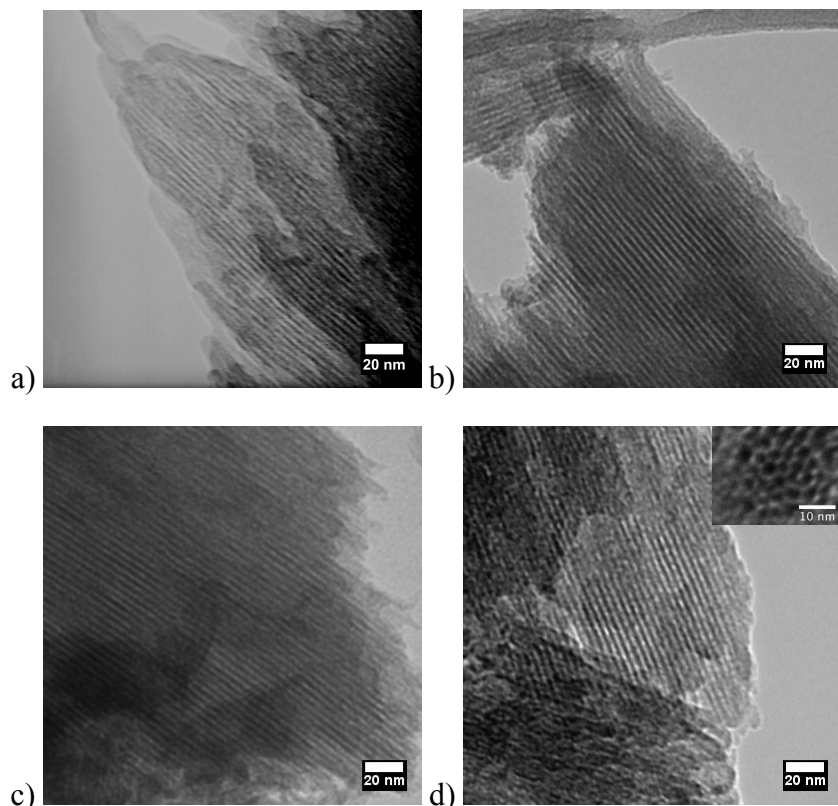


Figure S2. TEM micrographs of: a) PMO, b) NH₂-PMO, c) Alk-NH-PMO1 and d) Alk-NH-PMO2 (the inset displays a micrograph where the hexagonal arrangement of pores can be seen).

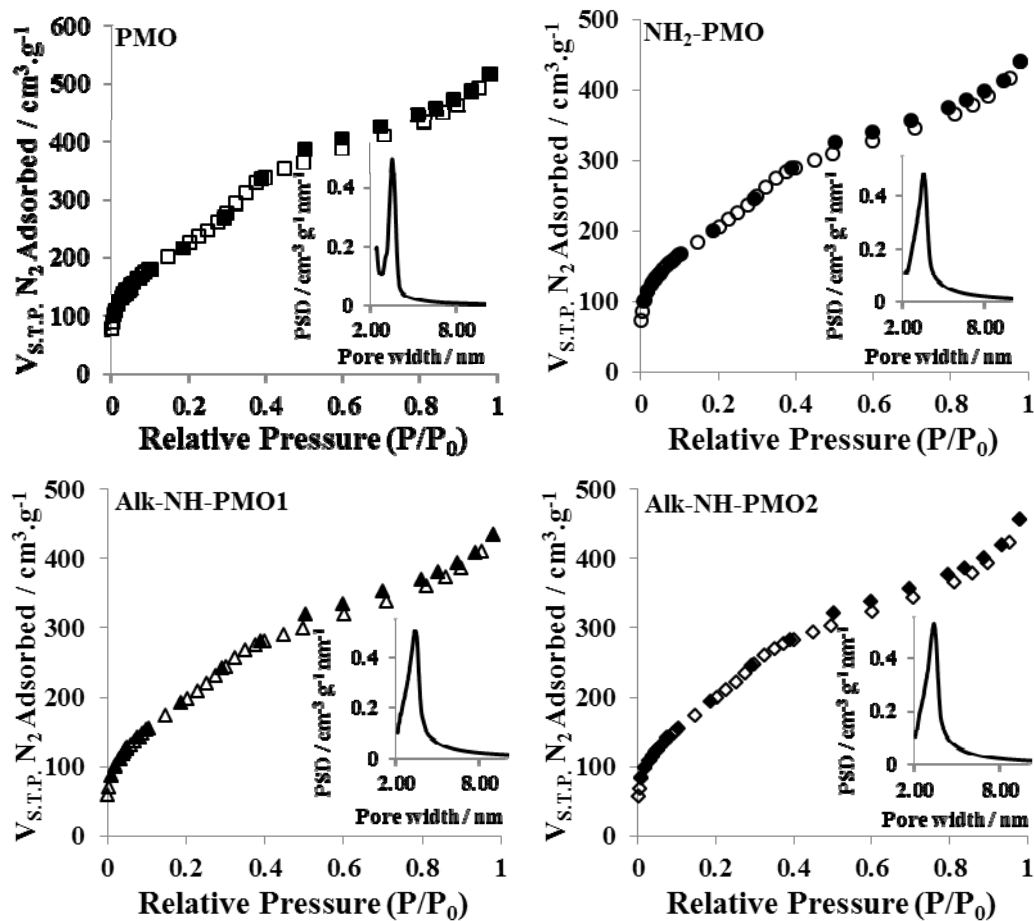


Figure S3. $-196\text{ }^{\circ}\text{C}$ N_2 isotherms of PMO ((□) adsorption; (■) desorption)), $\text{NH}_2\text{-PMO}$ ((○) adsorption; (●) desorption)), Alk-NH-PMO1 ((Δ) adsorption; (▲) desorption)) and Alk-NH-PMO2 ((◊) adsorption; desorption (◆)).

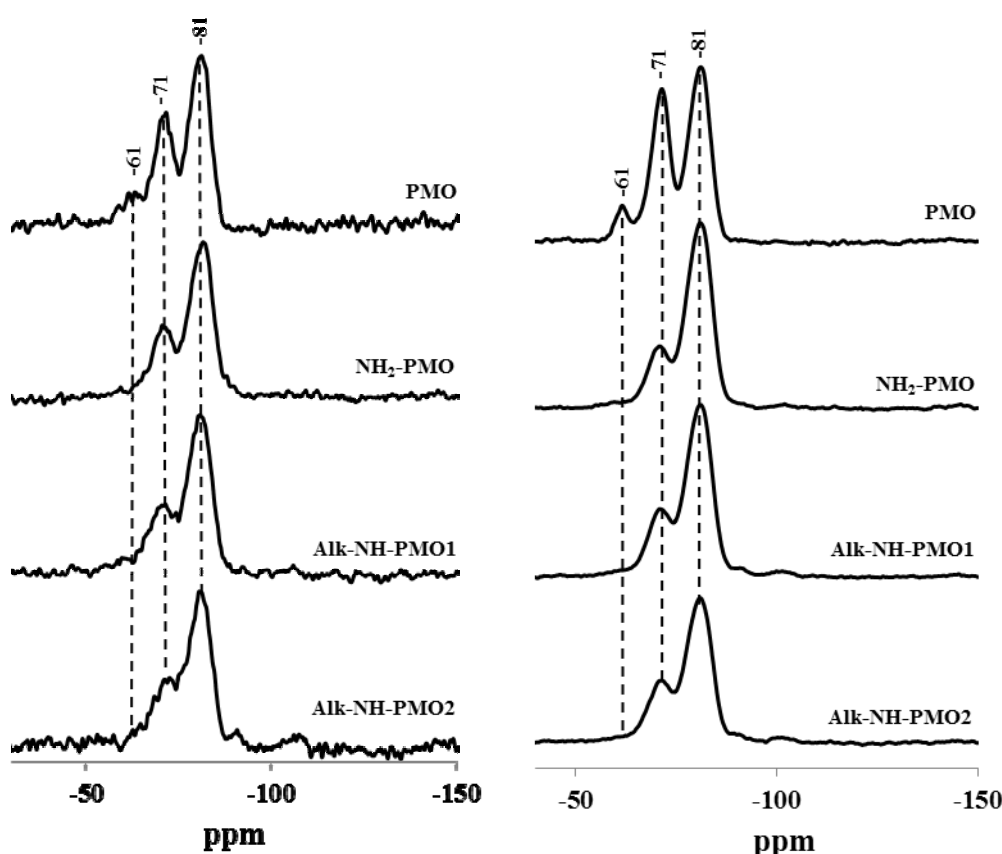


Figure S4. ^{29}Si MAS (left) and CP-MAS (right) NMR spectra of PMO, $\text{NH}_2\text{-PMO}$, Alk-NH-PMO1 and Alk-NH-PMO2.

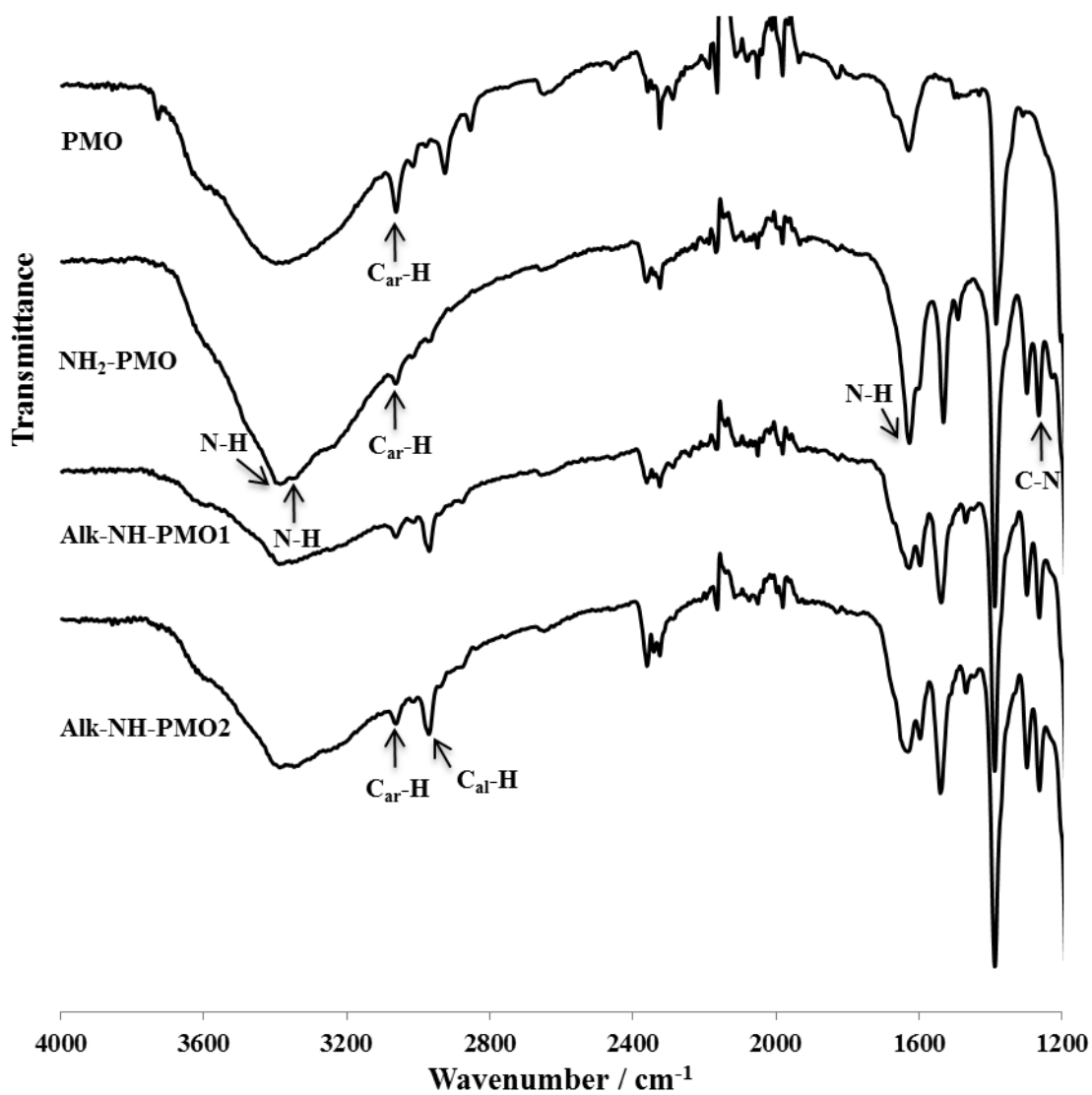


Figure S5. FTIR (ATR) spectra of PMO, NH₂-PMO, Alk-NH-PMO1 and Alk-NH-PMO2 in the range of 1200 - 4000 cm⁻¹ (C_{ar} and C_{al} despite for aromatic and aliphatic carbons, respectively).

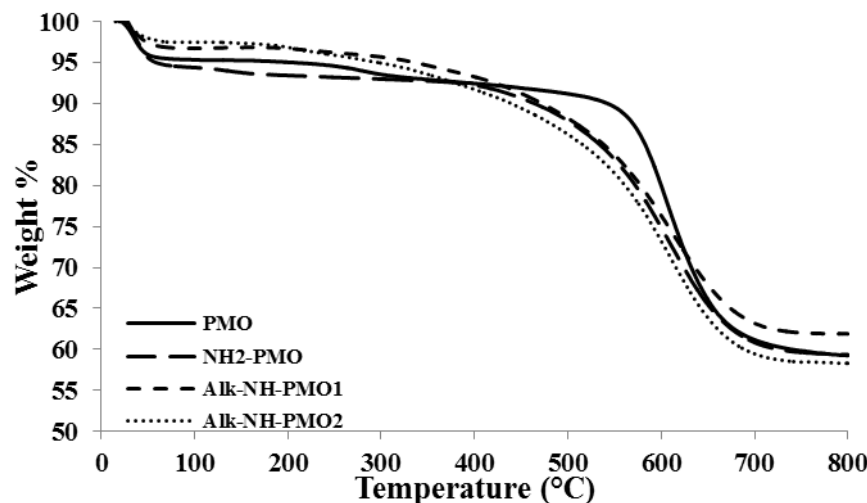


Figure S6. TGA of PMO, NH₂-PMO, Alk-NH-PMO1 and Alk-NH-PMO2.

Table S2. Elemental analyses of PMO, NH₂-PMO, Alk-NH-PMO1 and Alk-NH-PMO2.

Sample	% N	% C	% H
PMO	0.10	38.89	2.75
NH ₂ -PMO	3.03	35.81	2.92
Alk-NH-PMO1	2.96	37.50	3.37
Alk-NH-PMO2	3.00	38.05	3.44